

MSL DSENDS EDL ANALYSIS AND OPERATIONS

P. Daniel Burkhart⁽¹⁾ and Jordi Casoliva⁽²⁾

⁽¹⁾⁽²⁾*Jet Propulsion Laboratory, California Institute of Technology, 4800 Oak Grove Drive M/S 230-110, Pasadena, CA 91107, (818) 393-7939, dan.burkhart@jpl.nasa.gov*

⁽¹⁾*Mission Design Engineer, Guidance, Navigation and Control section*

⁽²⁾*Guidance and Control Engineer, Guidance, Navigation and Control section*

Abstract: *The most recent planetary science mission to Mars is the Mars Science Laboratory (MSL) with the Curiosity rover, which launched November 26, 2011 and landed successfully at Gale Crater on August 6, 2012. This rover was the first use at Mars of a complete closed-loop Guidance, Navigation, and Control (GN&C) system, including guided entry with a lifting body (via center of gravity offset) to greatly reduce targeting errors during the Entry, Descent, and Landing (EDL) phase. Hypersonic entry guidance enables the entry body to fly out the remnant delivery error from the final Trajectory Correction Maneuver (TCM) as well as other sources, resulting in less than a $25\text{ km} \times 20\text{ km}$ landing error relative to the Gale Crater landing target.*

This paper presents the operations experience of the JPL EDL trajectory simulation team, focusing on events in the week before landing and EDL itself. A brief description of the EDL trajectory simulation tool used for targeting and simulation verification analysis will be presented, including a high level discussion of the required modeling. Initialization and output interfaces used for landing hazard analysis will also be covered, along with discussion of real-time EDL event detection using radiometric Doppler data.

Keywords: *Mars Science Laboratory; Entry, Descent, and Landing; DSENDS Operations*

1. Introduction

The most recent planetary science mission to Mars is the Mars Science Laboratory (MSL) with the Curiosity rover, which launched November 26, 2011 and landed at Gale Crater on August 6, 2012. The MSL mission has four primary science objectives [1]; to accomplish these objectives, this rover has a significantly larger and more advanced landing payload than any previous Mars lander mission. The increased mass required a lifting entry body (via center of gravity offset) to ensure adequate Entry, Descent, and Landing (EDL) performance and timeline margins. In addition, MSL was the first use at Mars of a complete closed-loop Guidance Navigation, and Control (GN&C) system, including guided entry, to greatly reduce targeting errors during the EDL phase. The hypersonic entry guidance enables the entry body to fly out the remnant delivery error from the final Trajectory Correction Maneuver (TCM) along with aerodynamic and atmospheric uncertainties during EDL, resulting in less than a $25\text{ km} \times 20\text{ km}$ landing error relative to the Gale Crater landing target.

To achieve the above targeting criteria, high-fidelity simulation of approach and EDL is required, with the focus of this paper on the EDL phase. The tool used for approach TCM targeting and 6 degree of freedom (6DOF) EDL trajectory verification analysis is the *Dynamics Simulator for Entry, Descent and Surface landing* (DSENDS). DSENDS is a high-fidelity simulation tool from the Jet

Propulsion Laboratory's Dynamics and Real-Time Simulation Laboratory for the development, test and operations of aero-flight vehicles. DSEENDS includes the capability to model a rigid multi-body spacecraft with gravity, aerodynamics, sensors and thrusters. This capability is augmented for MSL with project-specific atmosphere, aerodynamics, sensors, thrusters and GN&C flight software to enable high-fidelity trajectory simulation.

This paper presents the operations experience of the JPL EDL trajectory simulation team, focusing on events in the week before landing and EDL itself. To provide context, an overview of the MSL project and the DSEENDS tool is covered first. Details of the added MSL-specific models are provided to define the simulation framework available for targeting, simulation and Monte Carlo analysis. Each of these three areas use the same DSEENDS simulation tool but have significant configuration differences that will be explored.

Targeting for cruise and approach maneuvers includes simulating the lifting nominal EDL trajectory in an in-plane open-loop EDL simulation mode and applying an offset between the cruise/approach and EDL reference trajectory planes to eliminate cruise stage recontact. Targeting also requires close integration with the maneuver design process, so the interface between the maneuver and EDL simulations is discussed. This open-loop EDL simulation is also used in a runout mode (vs targeting mode) for generation of Deep Space Network (DSN) station predictions for ground tracking of EDL.

A weekly process of cruise navigation and maneuver design with EDL targeting is performed to update the expected maneuver and entry conditions for EDL based on the latest DSN-based navigation solutions. In addition, high-fidelity EDL trajectory simulations are performed with these weekly solutions to supply trajectory and timing predictions of EDL events of interest.

In order to determine dispersions about the expected trajectory, a selected set of EDL simulation input parameters are dispersed and multiple EDL full-fidelity simulations are executed. The results of these simulations are used to define statistics about the expected trajectory, timing, and parameters of interest. These dispersed results provide a confirming simulation result for the prime MSL EDL simulation capabilities. Finally, other support functions such as onboard state initialization, landing hazard analysis and other post-processing are covered.

2. MSL EDL Overview

A graphic showing the series of EDL events for MSL is shown in Figure 1. In the minutes before atmospheric entry interface, the cruise stage with the cruise support hardware and cruise balance masses added to move the capsule center of mass to the axis of symmetry are separated. The resulting offset center of mass results in aerodynamic lift, which is utilized during the entry phase by a modified Apollo entry guidance algorithm. Entry guidance commands the capsule bank angle to control the range flown by modulating the vertical lift component to deliver the capsule to the desired parachute deploy location and velocity [2]. The onboard state required for closed-loop guidance is computed via inertial propagation of the ground-provided initial conditions using an inertial measurement unit (IMU). Shortly before parachute deploy, MSL performs the Straighten Up and Flight Right (SUFR) maneuver in which entry balance masses are separated to re-align the

capsule center of mass with the axis of symmetry and the parachute line of force. Deployment of the 21.5 m Viking-heritage disk-gap-band (DGB) parachute is commanded near Mach 2 based on navigated velocity. Once the system decelerates to around Mach 0.7 the heat shield is separated and a Ka-band narrow-beam Doppler altimeter/velocimeter begins collecting data. Once the onboard navigation filter converges to a solution using radar data, the eight throttle-able Viking-derived Mars Landing Engines (MLEs) are primed. The powered descent vehicle with the Curiosity rover attached separates from the backshell based on estimated altitude and velocity and performs an out-of-plane divert maneuver to avoid recontact with the backshell and then flies to a constant vertical velocity condition. The system has altitude margin built in to accommodate variations in both the terrain below the rover and measurement error. At a commanded altitude the rover is separated from the powered descent vehicle on a tether and the rover mobility is deployed for touchdown. The powered descent vehicle descends at a constant velocity until a persistent rover offloading is detected by GN&C. Once this has been detected, the tether is cut and the descent stage flies away to a safe distance [3].

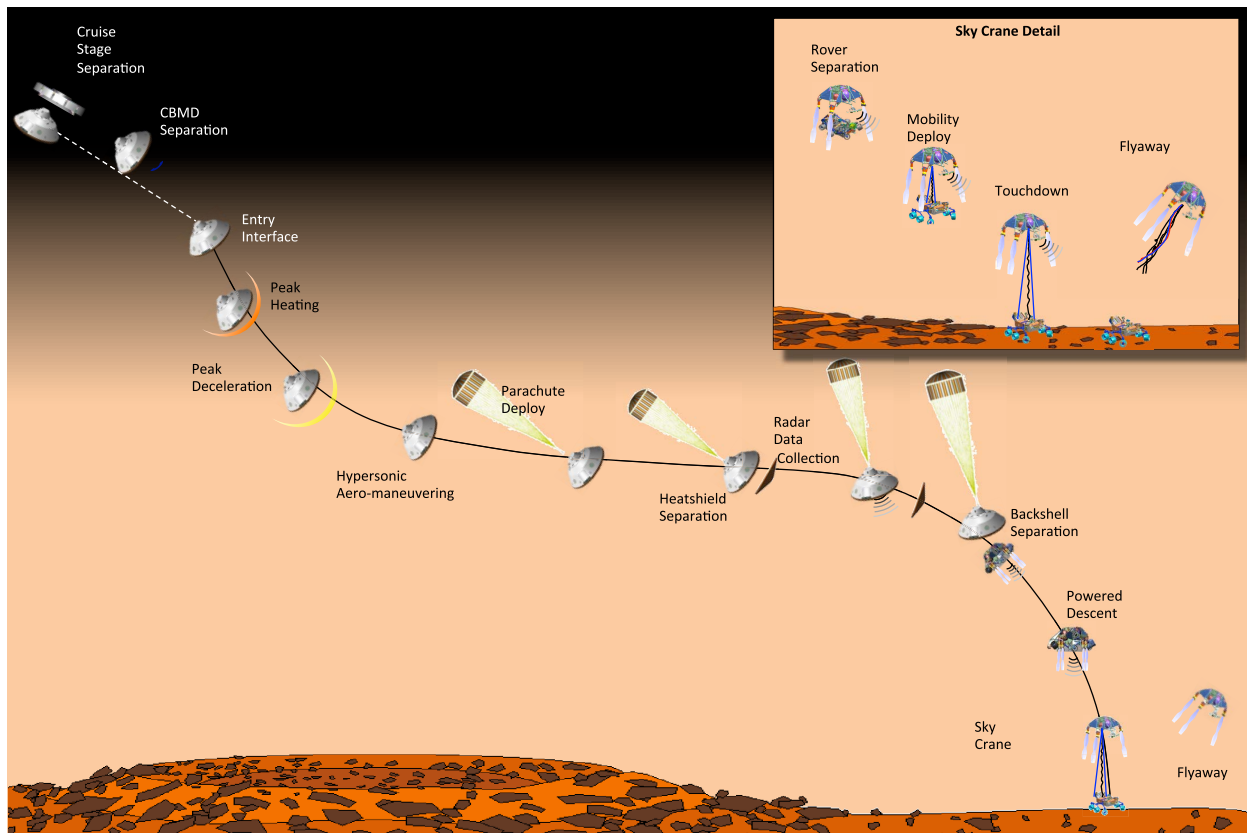


Figure 1. MSL Entry, Descent and Landing

3. DSENGS Description

The JPL MSL EDL trajectory analysis team had two major simulation actions for operations. The first was high-fidelity trajectory and simulation verification analysis of the POST2 simulation from the Langley Research Center, the primary performance simulation tool for MSL EDL analysis. This verification analysis required including the full suite of EDL simulation models including dispersed

inputs for Monte Carlo analysis of EDL. The second was EDL trajectory simulation to support cruise TCM targeting and maneuver design, which required modeling of the EDL dynamics without closed-loop GNC. Both are covered in the following section. The simulation chosen for MSL was DSENDS (Dynamics Simulator for Entry, Descent and Surface landing). DSENDS provides the framework for modeling various aero-assisted simulations (EDL, aerobraking and aerocapture) with varying complexity from simple systems with single bodies and 3 degrees-of-freedom (DOF) dynamics to multi-body, flexible systems. In addition to the framework and as-delivered models, several MSL-specific models were added to complete the simulation. All are covered below.

3.1. Inherited Capabilities

The simulation toolkit contains an extensive library of models for sensors (e.g. inertial measurement units, cameras, encoders), actuators (e.g. motors, thrusters, propellers), environments (e.g. atmospheric models, 2.5- and 3-dimensional terrain models), environment interaction (e.g. wheel slip, vehicle flight), and avionics elements (e.g. communication devices). A number of common control and navigation functions are available as well to close the loop in the absence of a user-supplied model, while providing a framework for the easy linking of user-supplied code such as control, estimation and sensor routines. A state-machine orchestrates mode and event-related functions including the activation and de-activation of elements in the data-flow. The simulation also provides an automated Monte Carlo, parametric simulation capability allowing automated dispatch of jobs onto computing clusters. In addition to the core simulation capabilities, a multi-stream continuous and event data logging facility is provided to facilitate data gathering. For the MSL EDL simulation, several project-specific modules were added, as described below.

3.2. MSL Device Models

MSL-specific device models for the inertial measurement unit (IMU) and RCS thrusters were integrated into DSENDS. Both models were built and maintained by the EDL GN&C team and source code was delivered to the simulation teams for integration. The GN&C team was responsible for unit and performance testing of the models. The GN&C team worked both with the hardware developers to verify the models performed as expected and with the DSENDS team to ensure the inputs supplied to the models were correctly defined and that the implemented model operated correctly within the simulation. Input and sign-off from all three groups was required to certify the IMU and RCS thruster models for operations use.

3.3. MSL Flight Software

The MSL EDL GN&C flight software was integrated into the high-performance EDL simulations. This includes the core EDL GN&C functionality along with the EDL timeline engine to model the real mode changes of the spacecraft. The inputs to the flight software are initialization data and sensor data from the IMU during operation. Outputs from flight software are messages reporting data of interest, commands to fire the RCS thrusters and commands to fire various pyrotechnic devices for separations, ejections and propulsion system pressurization. Working with the GN&C team, the DSENDS team verified the proper operation of flight software in the simulations, proper input of sensor data, and proper simulation responses to all flight software output.

3.4. MSL Atmosphere and Aerodynamics Models

The Martian atmosphere, including atmospheric density, temperature, winds and dispersion of these quantities, was modeled using mesoscale-derived atmosphere tables with final dispersed atmospheric quantities computed using a modified version of MarsGRAM 2005 [4]. A software subroutine was delivered to model the blunt-body nominal and dispersed capsule aerodynamics. Verification included confirming the proper atmosphere and capsule state information was passed to the model and that the proper aerodynamics coefficients were computed based on the simulation inputs. Data were generated by the implemented model and passed to the model developer to confirm the proper output for both nominal and dispersed cases [5].

3.5. MSL Parachute Model

MSL used a supersonic Disk-Gap-Band (DGB) parachute during its EDL sequence. Thus far, every robotic mission to Mars has used heritage from the deceleration technologies developed during the Viking era in the 1960s. The MSL DGB parachute had a 33% larger diameter than the Viking parachute due to the heavier weight of the MSL spacecraft during EDL. The MSL parachute model includes tabular aerodynamic properties both as a function of parachute angle of attack and Mach number, a set of mass properties for the mechanical framework of the parachute and an area oscillation model that is active above Mach 1.4.

The supersonic MSL parachute consists of a parachute canopy, riser, confluence fitting and triple bridle legs as shown in Figure 2. The canopy and riser are modeled as a single rigid body with composite mass properties. The triple bridle attached to the capsule backshell is modeled as a single line rigidly attached to the backshell. The bridle and riser are connected by a ball joint, with all other joints shown in Figure 2 modeled as rigid links [6].

3.6. EDL trajectory nominal runs

Nominal EDL runout trajectories are simulated from the Entry interface minus 9 minutes (E-9min) to touchdown each time a new orbit determination (OD) solution is computed. As MSL is cruising towards Mars, better state estimates are obtained and the propagated state of the spacecraft at E-9min varies. Thus, nominal runout simulations are used to quickly evaluate the sensitivity of state variation at E-9min with respect to the rover position at touchdown.

The EDL simulation output was used to create trajectory data products that were used for subsequent analysis. Each trajectory data product included the EDL simulated trajectory along with an approach trajectory segment until E-9min and a 10 minute segment that contained the touchdown position coordinates representing the static rover on the surface of Mars. The added segments were included on both ends of the EDL runout trajectory to allow the orbiter phasing and communication analysis [7] to query trajectory state and attitude values before, during and after the EDL runout trajectory.

For each navigation solution, three EDL runout nominal trajectory files were generated with varying simulation fidelity. The main trajectory output was from the high-fidelity 6-DOF EDL simulation,

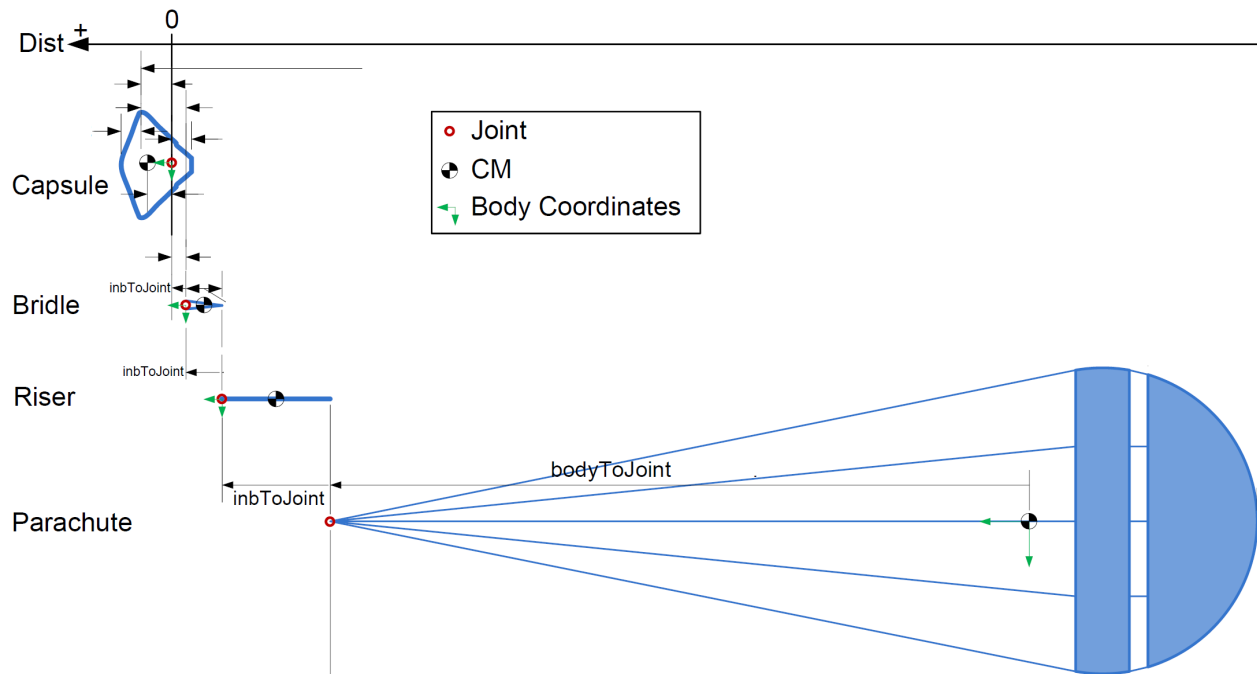


Figure 2. MSL DSENGS simulation body diagram for the parachute phase.

used to compute the mapping between the spacecraft state at E-9min to touchdown. This output is used both for landing hazard analysis, discussed later, and to evaluate the need to update the onboard EDL flight software parameters. In addition, time histories of position, velocity and attitude were used to analyze [7] the phasing of Mars Reconnaissance Orbiter, Mars Odyssey, and Mars Express with respect to MSL.

In addition to the full-fidelity 6-DOF EDL trajectory, two 3-DOF EDL trajectory runouts were also created using the targeting simulation, one with a complete sequence of EDL events and another that does not include parachute deploy or events after parachute deploy. The full-fidelity output was used to evaluate potential shifts on the touchdown ellipse so that hazard analysis could be performed and the probability of mission success could be computed. The 3-DOF output was used as the input trajectory models for EDL radiometric Doppler analysis.

3.7. EDL trajectory simulation for targeting

For previous direct-entry missions to Mars, a single full-fidelity simulation tool for EDL could be used to model EDL for all required analyses, including trajectory runout, Monte Carlo analysis and cruise TCM targeting. These previous missions are similar in that there is no active closed-loop control of the EDL trajectory: the exception is the use of ground sensing of altitude and/or velocity for powered flight and other event triggers, but these uses were not to control the trajectory back to a defined reference trajectory or landing location.

The story for MSL is different due to the designed offset of the center of mass from the capsule axis of symmetry, resulting in lift. Lift was used by the Viking landers to increase the altitude of parachute deploy and thus improve timeline margin and increase the delivered mass capability, and

was included on MSL for similar reasons. In addition MSL included closed-loop entry guidance as discussed earlier. In addition to the above improvements, entry guidance will command the capsule bank angle to adjust the vertical lift of MSL to control both range remaining to the parachute deploy target and reduce errors in cross range so the entry trajectory flies over the parachute deploy target, resulting in significant improvements to landing accuracy. The desired trajectory conditions as a function of velocity are included in flight software as a reference table that is used by entry guidance to compute the commanded bank angle. While entry guidance can correct a range of initial condition error, the goal of the targeting process is to achieve the EDL initial conditions that match the reference EDL trajectory to preserve entry guidance capability to correct trajectory errors as margin. As such, for cruise TCM targeting, a simulation capability that does not include closed-loop guidance but simply executes the reference profile is required, as otherwise the guidance will use its control authority to remove position errors due to initial condition errors.

To support this, a second MSL simulation configuration was developed, referred to as the open-loop simulation. Starting with the full fidelity simulation used for nominal EDL runouts described above, several capabilities were modified. First, the the closed-loop control of the lift vector has been disabled. This is replaced by defining a profile of vertical lift desired as a function of velocity to shape the entry trajectory for optimal performance, with this lift profile specified using a bank angle profile. This is implemented for the open-loop simulation by prescribing the lift to be applied only in the vertical direction and decrementing the magnitude based on the bank angle profile. In other words, the lift direction is defined by the bank profile and projected into the vertical plane for integration in the capsule dynamics. Second, the angle of attack and sideslip angles during entry are computed using trim aerodynamics, as opposed to being governed by the rotational equations of motion in the full-fidelity simulation. Finally, the open-loop simulation is embedded in a wrapper function that translates the miss distance on the ground to changes in the entry interface initial conditions [8]. This EDL open-loop simulation is then executed in conjunction with a cruise maneuver design simulation, with iteration between the cruise maneuver and EDL simulations done until a single trajectory with a TCM propagates to the landing target within a specified tolerance.

3.8. Cruise Stage Recontact

As part of the project formulation phase, analysis of recontact between ejected elements and the main body of interest was done. For all Mars direct-entry landers to date, a separate cruise stage is attached to the entry body and jettisoned shortly before atmospheric entry. For a ballistic case, it can be shown that the separation relative velocity will put the entry body and capsule in slightly different orbit planes, making the likelihood of recontact very small. For MSL with closed-loop entry guidance, the entry body could cross once or more in front of the ejected cruise stage or cruise balance masses. While the analysis performed concluded the likelihood of recontact was negligible for the cruise balance masses, the situation with the cruise stage and its components as it broke apart was less clear cut.

To eliminate the admittedly low recontact probability, an offset was applied between the orbit planes for the approach trajectory and the open-loop EDL trajectory as part of the maneuver design targeting process. This would further move the trajectory plane for the ejected cruise stage from the EDL reference trajectory plane that's used as a reference for removing cross-range errors via bank

reversals. The magnitude of the offset was chosen to be within the expected cross track excursion based on the out-of-plane dead bands for bank reversals, meaning the offset was accounted for during EDL completely within the entry guidance corridor and system design and was achieved essentially for free.

4. Initialization

The high-fidelity EDL simulation has over 30,000 parameters that must be specified for proper operation. A large subset of these parameters, over 90% of the total, were either managed by an EDL configuration control spreadsheet or were parameters that were compiled into the software. The EDL configuration control spreadsheet values were mostly parameters related to models that did not have MSL-specific code provided, such as body geometry, thruster and IMU locations and orientations and antenna location and bore sight values. Values coded into the MSL-delivered RCS, IMU and flight software modules were both data from model performance verification but also configuration choices.

The remaining 10% of the parameters can be divided into two groups. The first group are flight software parameters that had a defined update mechanism based on binary files that could be supplied to the flight vehicle and ground simulation tools to maintain a consistent setup between flight and ground. Updates to these values were managed by the flight operations process and configuration management of the active parameter files, with the ground simulation inputs updated as required when the flight values were modified. The second group are the set of parameters that are most likely to change or are planned to be updated during late approach. This group includes the EDL GN&C trajectory initial conditions (position, velocity, attitude and time), landing site latitude and longitude coordinates, entry guidance initial commanded bank angle, expected range flown from parachute deploy to landing and post-landing descent stage flyaway direction. This set of parameters was captured in the EDL Parameter Update File (EPUF).

The EPUF was used both to update the flight vehicle state and to initialize the ground simulation parameters listed above. The file was generated using an automated process that took as input the best estimated approach trajectory of MSL and a handoff configuration file. Since the best estimated approach trajectory changes every time new DSN tracking data are processed by the navigation team, a series of distinct update opportunities were defined based on the expected navigation performance and available opportunities to command the spacecraft. The handoff configuration file was the source for the remaining planned update parameters. This file was reviewed and updated as needed within the flight operations process for evaluating changes to the onboard parameters, with the values captured in this file as the source for the uplink products that were created and the source for the ground simulation inputs.

5. Landing hazard analysis

Once the EDL Monte Carlo simulations are executed, post-processing tasks including landing hazard analysis are performed to quantify the probability of a successful landing, accounting for landing site terrain hazards. The analysis performed for MSL began with the collection and processing of imaging from the High Resolution Imaging Science Experiment (HiRISE) on MRO. HiRISE

images allowed for characterization of the local surface topography at length scales smaller than the Curiosity rover. Combined with the smaller landing ellipse due to guided entry, the project was able to characterize the entire expected landing terrain for the first time in the history of planetary exploration. The product of this work is a hazard map that defines the probability of a landing failure due to various terrain-induced mechanisms [9].

The mechanism for reporting landing hazards was revolutionized by the 2007 Phoenix lander with the computation of landing hazards at the pixel level versus the definition of hazard regions as was done for Mars Exploration Rover (MER) and Mars Pathfinder. A similar pixel-based approach was used for MSL as well to define the hazard maps. With these data, the process used to compute landing success probability was to convolve the probability of landing at a particular location based on Monte Carlo analysis from the high-fidelity EDL simulation discussed earlier with the probability of the location having a hazard that causes a landing failure. The tool used for this analysis, as for previous missions, was MarsLS [10].

The combined hazard map for MSL's Gale landing site is shown in Figure 3, including the landing target, a science drive target used to help place the ellipse and three landing ellipses. These landing ellipses were computed based on varying EDL dispersions to capture a case without added uncertainty to represent a best-case uncertainty (the "lower bound"), a case with the pre-landing agreed-to uncertainties associated with EDL (the "best estimate") and a case with larger than expected uncertainties (the "upper bound"). These three ellipses are of interest for different reasons: a larger ellipse will be more likely to intersect with areas of high probability of failure and tend to have higher failure probabilities in a broad sense, but the smaller ellipses will have higher failure probabilities for specific hazards since the total hazardous area is larger relative to the ellipse size.

With the data for both the Monte Carlo landing location and the landing hazard map, the probability of a successful landing can be computed using MarsLS. However, one additional change to the convolution was made. The convolution process in the past assumed the Monte Carlo landing points represent a bivariate Gaussian ellipse. Since the hazard map data are defined at the pixel level and the Monte Carlo data are ingested as the Monte Carlo landing points, the capability to compute the probabilities using the points directly was added to the MarsLS tool. One concern with this approach is the variation that occurs with small hazards that may or may not be hit by a particular point but are within the cloud of points, resulting in some variation in the probability computed.

To address this concern, the capability of MarsLS to take an input landing dispersion and translate the distribution accurately across the map was used both with the new points-based distribution and the original ellipse-based distribution. At each location the total probability of successful landing was computed. This process was repeated, moving the landing point center to each pixel in the hazard map and computing the resulting probability of success. These data were then plotted on a contour map as shown in Figure 4 for both the points and ellipse assumptions. The map represents the probability of successful landing on the MSL hazard map with a specified landing points file centered at the reported latitude and longitude point. By comparing these maps, it can be concluded that the MSL landing points distribution is strongly bivariate Gaussian and that the sparsity of points versus the gap-free coverage of the ellipse does not introduce a significant error to the total probability of success calculation. Since the ellipse based maps result in smoother contours and this

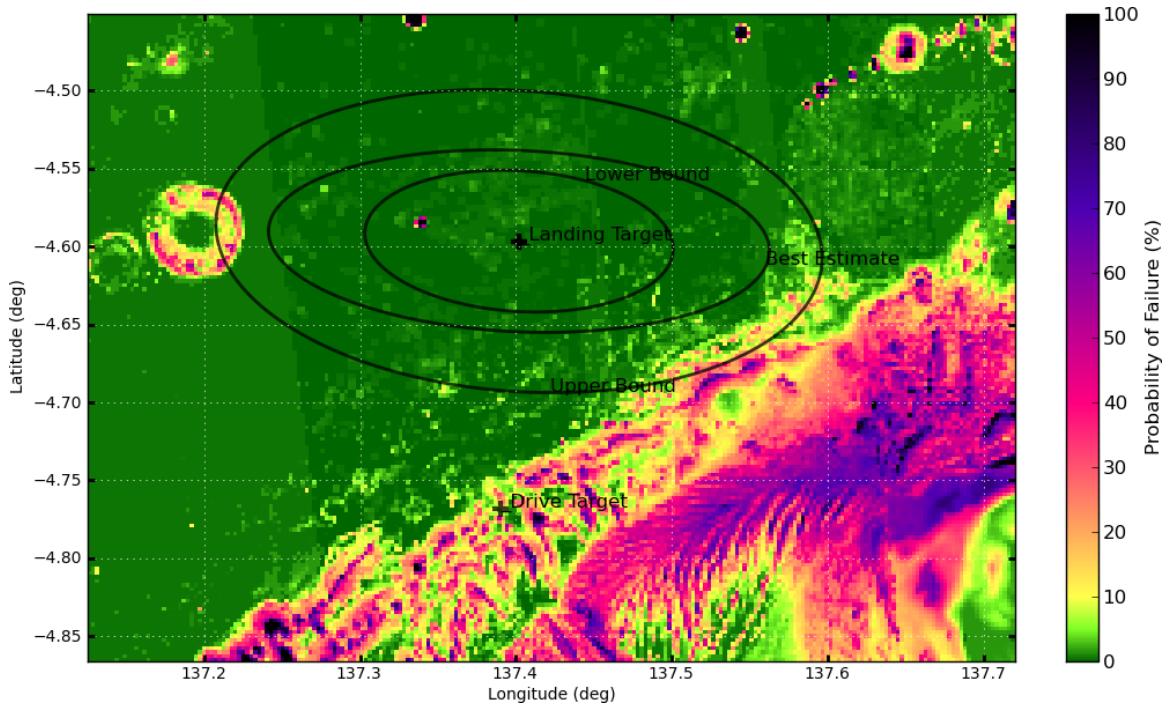


Figure 3. Combined hazard map showing the best estimate, lower bound and upper bound landing ellipses

are easier to read, subsequent maps will be computed using the ellipse method.

One use for the above contour map was to capture the expected success probability as a function of ellipse centers to enable the use of single high-fidelity simulation runs that represent the expected Monte Carlo mean landing location to get expected landing success numbers without running full Monte Carlo analyses. This was especially useful in the final days before EDL, where time for full Monte Carlo analyses was not available. To create the contour map, total probability of success maps were first created for each of the ellipses shown in Figure 3. These three contour maps are then compared at each pixel and the maximum value for each corresponding pixel is selected for use in the final map. This will capture both the higher broad-scale probability of failure and the smaller-scale peak failure values that result from the smaller ellipse. The resulting contour map is shown in Figure 5 along with the landing target and drive targets shown before.

An example showing some runout cases from both the primary (POST2) and verification (DSENGS) performance simulations is shown in Figure 6, which is the same contour map as in Figure 5 but zoomed in to show the runout cases. The EDL initial conditions are based on cruise navigation solutions based on tracking data cutoffs at various times during the last three days of cruise and propagated to the EDL simulation start time [11]. As discussed above, these points represent the center points of Monte Carlo ellipses with the contour value at each point equal to the probability of successful landing for that ellipse. These data show that the expected landing location did change with time but that the impact of that change on the computed landing success probability was within 0.1%, which is within the confidence interval for the hazard map data and thus statistically equivalent.

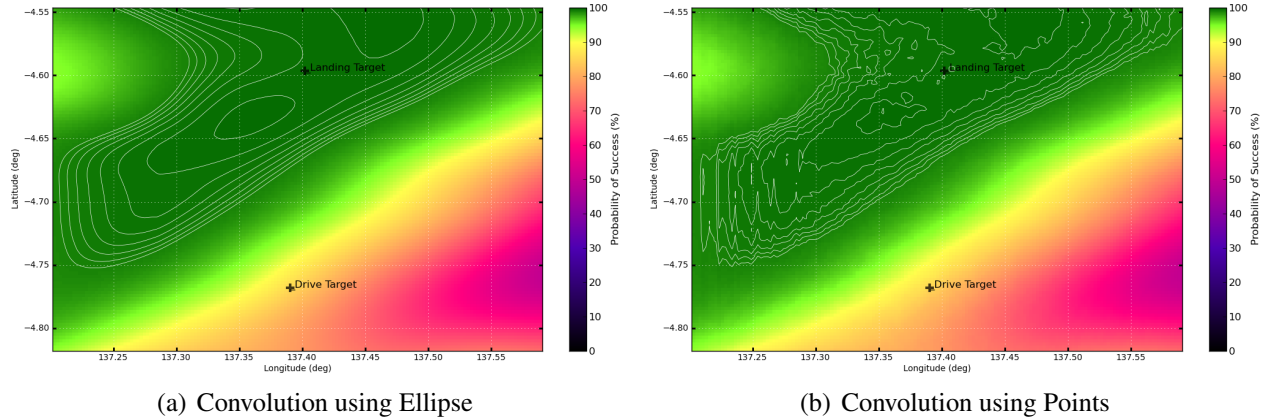


Figure 4. Comparison of hazard map convolution with ellipse computed based on the dispersed landing points and with the raw dispersed landing points. The white contour lines represent changes in probability of success in 0.1% increments.

6. Real-time Doppler

One responsibility of the JPL EDL simulation team during the EDL event itself was to monitor the real-time radiometric data to detect EDL events. Events that impart a significant velocity change along the Earth line will be visible as discontinuities or slope changes in the Doppler data. This includes known events, such as separations and ejections of mass, antenna changes, thruster activity, drag due to atmospheric entry and parachute deploy as well as unexpected velocity changes.

The process is set up as follows: The radiometric Doppler data from the Deep Space Network (DSN) tracking stations is streamed in real time to a navigation server. This server has a Doppler prediction based on a simulated trajectory of MSL that is used to compute the difference between the observations and the computed Doppler measurement (Doppler residual). These Doppler residuals are available for display and were monitored during EDL for event detection. A set of events of interest is listed in Table 1. Note that occultation due to loss of line-of-sight between Earth and MSL occurs shortly after heat shield separation, but subsequent events of note are included in the table for completeness.

Exo-atmospheric events of interest are shown in the two plots in Figure 7. The first shows venting of the cruise heat rejection system (HRS) coolant, a required event before separating the cruise stage. The Doppler residual show a total shift of approximately 4 Hz , which is a line-of sight velocity change of 70 mm/s . The second shows the Doppler residuals continuing through atmospheric entry. In time order, the first event of note is a gap in the Doppler data due to setup of X-band tones, which also reinforces the parachute low gain antenna (PLGA) X-band antenna configuration and causes the resulting gap. The next event is cruise stage separation, which is shown in the inset figure and corresponds to the expected event time from Table 1. The residuals show a shift of approximately 2.5 Hz , which is a line-of-sight velocity change of 45 mm/s . The next expected event is the activation of EDL GN&C which starts a series of entry reaction control system (RCS) thruster warm-up firings and executes a despin and turn to the entry attitude. Unfortunately, for an as-yet-unexplained reason, the Doppler data has a gap that starts shortly before GN&C start

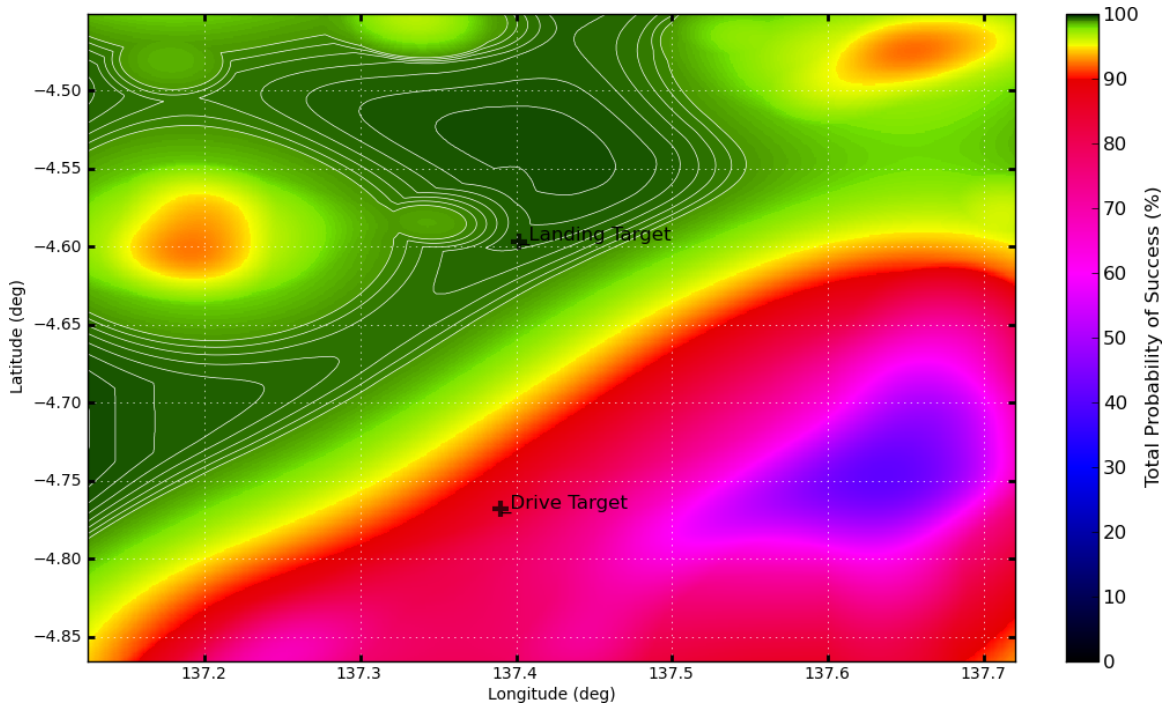


Figure 5. Total probability of success map based on the best estimate, lower bound and upper bound landing ellipses. The white contour lines represent changes in probability of success in 0.1% increments.

and ends after the expected end of the despin and turn-to-entry maneuvers. The GN&C start time is noted in the figure despite the lack of data. The final event of note is a short gap right before entry interface, which corresponds to another antenna swap, this time to the tilted low-gain antenna (TLGA), which is oriented to be near the anti-velocity direction of the entry lifting body. This alignment reduces the Doppler signature from entry phase bank reversals due to antenna motion.

For MSL operations on landing day, three EDL simulations of increasing fidelity were used to define the computed Doppler measurements used to build Doppler residuals. The first and lowest fidelity was a case without Mars atmosphere, which will show large-scale dynamic events but is too coarse to see any other EDL events. Residuals using this prediction were the main Doppler residual display shown to the public, as they do not assume any EDL events and are the easiest to predict. The residuals for this case from entry through Earth occultation are shown in Figure 8. The deceleration due to the atmosphere is readily apparent, as is the parachute deploy, both of which are noted.

The second higher-fidelity case includes the atmosphere and models the entry phase using the open-loop setup described before, which models atmospheric drag and vertical lift but does not include out-of-plane lift. This case also did not model the parachute deploy or any other events after parachute deploy (no heat shield release or powered flight) but instead models flight in the capsule configuration to impact. These residuals are shown in Figure 9. These residuals, unlike those in Figure 8, do not show a large drag signature. With much of the drag modeled in the prediction, the differences in the model here appear to be small, as shown by the lack of a large upward or

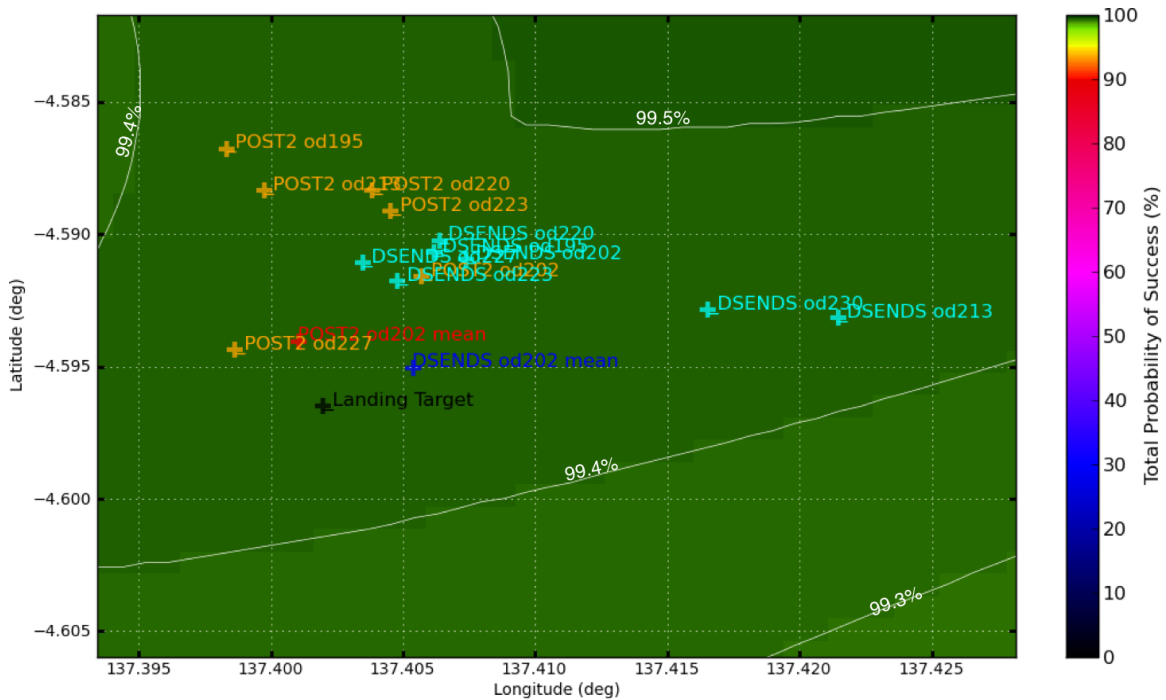
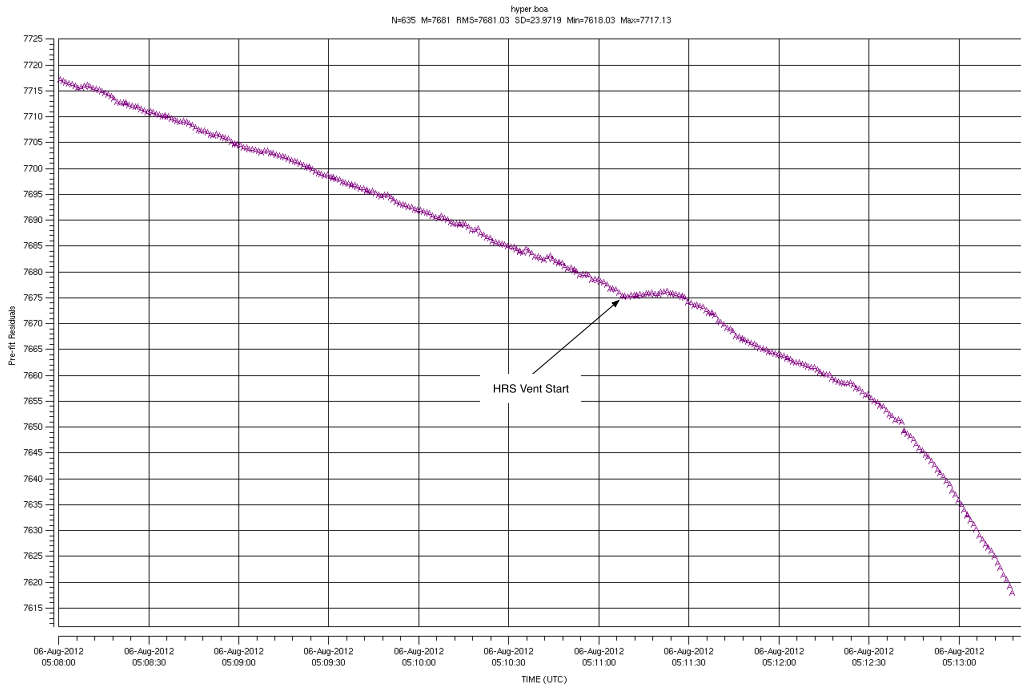


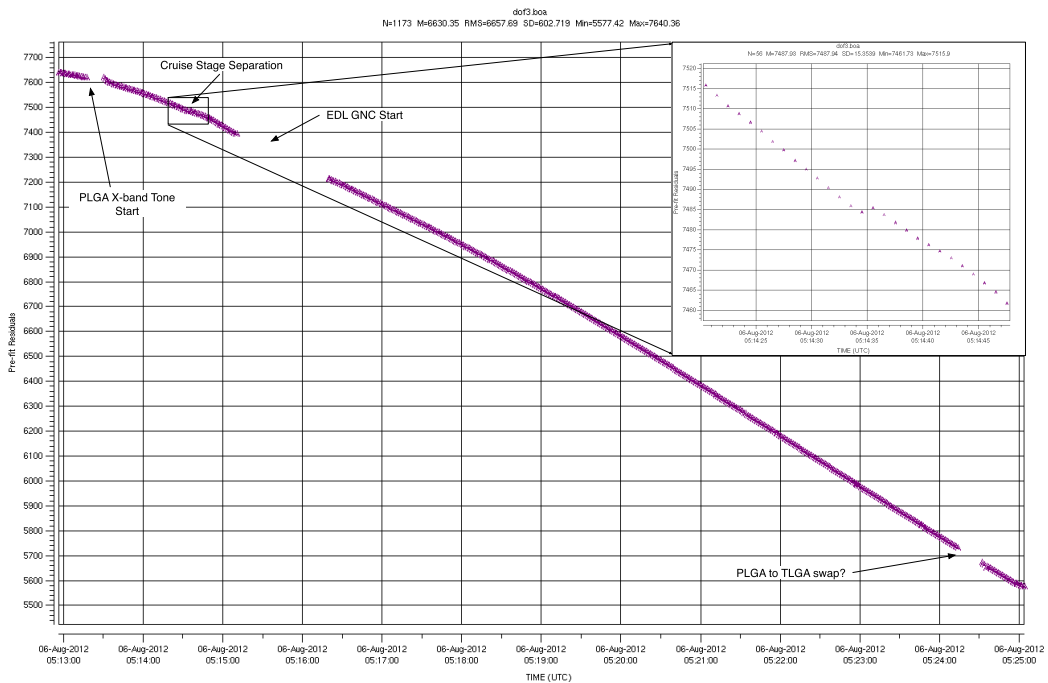
Figure 6. Nominal trajectory landing locations by ground navigation solution number. The tics are roughly 300m apart. The red and green points represent the centers of full Monte Carlo analyses from both EDL simulations.

downward trend change relative to the exo-atmospheric data in the plot. With the majority of capsule drag and vertical lift removed, the impact of bank reversals in guided entry are large signatures, with the changes mostly due to the lift-induced velocity changes since there are no discontinuities corresponding to turn-induced antenna motion effects of the reversal but smooth rate changes through the three bank reversals. Due to the well-modeled drag, the SUFR turn can be seen in the data as well. A much larger discontinuity due to parachute drag relative to the no atmosphere case and the signature for the heat shield release can be seen as well. Overall this prediction worked the best for showing dynamic events of interest, mostly due to the good prediction of the capsule drag. If the drag model were significantly off, there would have been a larger offset due to atmospheric entry and subsequent obfuscation of the events shown here.

The third and highest-fidelity case includes the complete 6-DOF model of EDL, with all events and deployments included. The predicted trajectory for this case uses the same EDL GN&C parameter update that's active on the spacecraft, while the simulation truth initial conditions are based on the latest available navigation predicted trajectory. These residuals are shown in Figure 10. The bank reversal signature in the residuals is reasonably clear but some timing and magnitude variations are apparent in the signature. It is also clear from the residuals that the modeled parachute deploy is several seconds earlier than the actual parachute deploy, as seen by the sharp positive then negative signature, as noted in the figure. Further investigation is in progress to determine the cause for this and other differences in the prediction relative to flight data. In addition to the heat shield release signature there are some other variations in the Doppler that will require a more detailed reconstruction to resolve.



(a) HRS Vent



(b) GNC start to entry interface (inset: cruise stage separation)

Figure 7. Real-time Doppler for exo-atmospheric events of interest

Table 1. Event times for selected EDL Events based on flight software reported values, shown in UTC at the spacecraft and corrected for one-way light time to Earth.

Event Name	Spacecraft Time (UTC, 06-AUG-2012)	Earth Receive Time (UTC, 06-AUG-2012)
Cruise Stage Separation	05:01:53	05:14:34
T0 GNC Start	05:02:53	05:15:34
Entry Interface	05:11:53	05:24:34
Entry Guidance Start	05:12:39	05:24:34
Start Bank Reversal 1	05:13:06	05:25:47
End Bank Reversal 1	05:13:18	05:25:59
Start Bank Reversal 2	05:13:27	05:26:08
End Bank Reversal 2	05:13:37	05:26:18
Start Bank Reversal 3	05:13:56	05:26:37
End Bank Reversal 3	05:14:07	05:26:47
Start Heading Alignment	05:14:09	05:26:49
SUFR/EBM Ejection	05:15:53	05:28:34
Parachute Deploy	05:16:12	05:28:53
Heat Shield Release	05:16:32	05:29:13
DTE Mars Occultation	05:17:01	05:29:42
Backshell Separation	05:18:09	05:30:50
Rover Touchdown	05:19:05	05:31:46

7. Acknowledgements

The authors would like to acknowledge the contributions of Tomas Martin-Mur, the MSL navigation team chief, to the processing of hazard map files and the plotting tools used for the landed graphics shown in this paper. We also thank the DSENDS simulation developers Bob Balaram, Christopher Lim, Jonathan Cameron and Kam Tso for their support both for software and for user support.

This research was carried out at the Jet Propulsion Laboratory, California Institute of Technology, under a contract with the National Aeronautics and Space Administration.

8. References

- [1] Baker, C. J. "Mars Science Laboratory Mission Plan Revision C (Pre-Launch Final)." Project Document JPL D-27162, Jet Propulsion Laboratory, May 15 2011.
- [2] Mendeck, G. and Craig, L. Entry Guidance for the 2011 Mars Science Laboratory Mission. American Institute of Aeronautics and Astronautics, 2012/09/20 2011. doi: 10.2514/6.2011-6639.
- [3] Prakash, R., Burkhart, D., Chen, A., Comeaux, K., Guernsey, C., Kipp, D., Lorenzoni, L., Mendeck, G., Powell, R., Rivellini, T., Martin, M. S., Sell, S., Steltzner, A., and Way, D. "Mars Science Laboratory Entry, Descent, and Landing System Overview." "Proceedings of

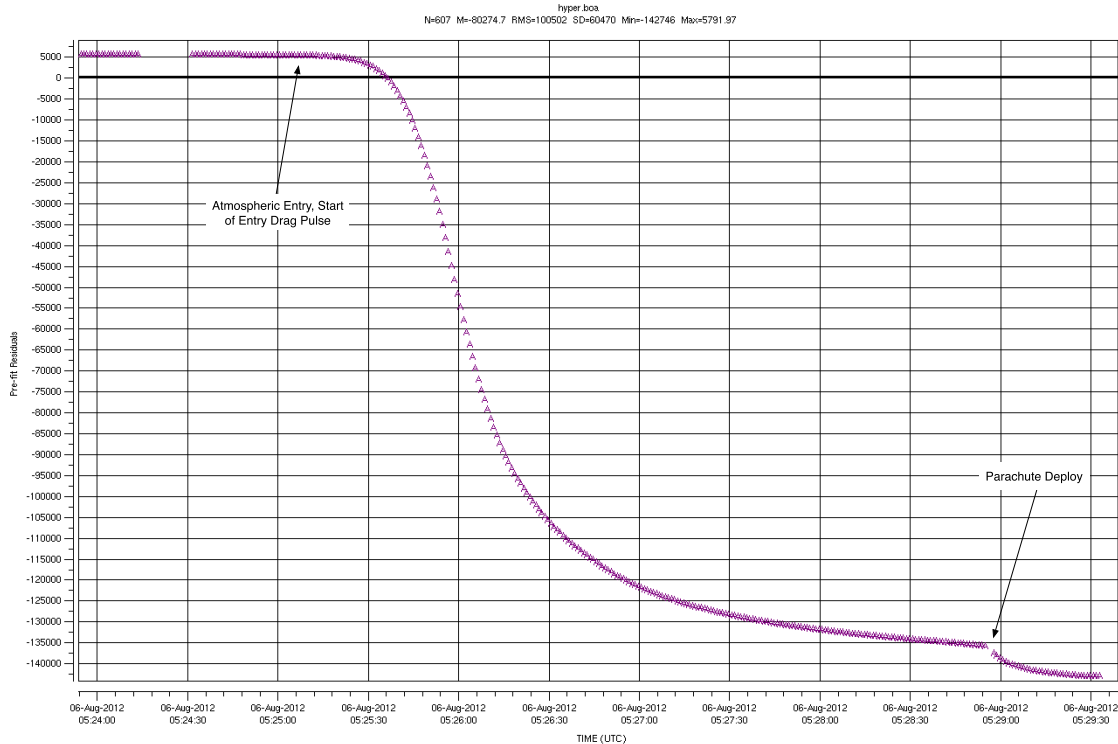


Figure 8. Real-time Doppler from entry to occultation, prediction without atmosphere. The start of the entry drag pulse is noted, along with parachute deploy

the 2008 IEEE Aerospace Conference,” p. 18 pp. IEEE 10.1109/AERO.2008.4526283, Big Sky, MO, Mar. 1-8, 2008.

- [4] Chen, A., Vasavada, A., Cianciolo, A., Barnes, J., Tyler, D., Rafkin, S., Hinson, D., and Lewis, S. “Atmospheric risk assessment for the Mars Science Laboratory Entry, Descent, and Landing system.” “Aerospace Conference, 2010 IEEE,” pp. 1 –12. march 2010. ISSN 1095-323X. doi:10.1109/AERO.2010.5447015.
- [5] Schoenenberger, M., Dyakonov, A., Buning, P., Scallion, B., and Norman, J. V. “Aerodynamic Challenges for the Mars Science Laboratory Entry Descent and Landing.” “41st AIAA Thermophysics Conference,” AIAA, 2009. doi:10.2514/6.2009-3914.
- [6] Cruz, J., Way, D., Shidner, J., Davis, J., and Kipp, D. “Description of the Parachute Models Used in the POST End-to-End Simulation.” Mars Science Laboratory Internal Report. 2011.
- [7] Abilleira, F. and Shidner, J. “Entry, Descent and Landing Communications for the 2011 Mars Science Laboratory.” “AAS/AIAA Spaceflight Mechanics Meeting,” pp. 1–10. Kauai, Hawaii, February 10-14 2013.
- [8] Cook, R. “Preliminary Trajectory Targeting for Direct Entry Earth-Mars Trajectories.” In-office Memorandum 312/91.2-1832, Jet Propulsion Laboratory, September 3, 1992.

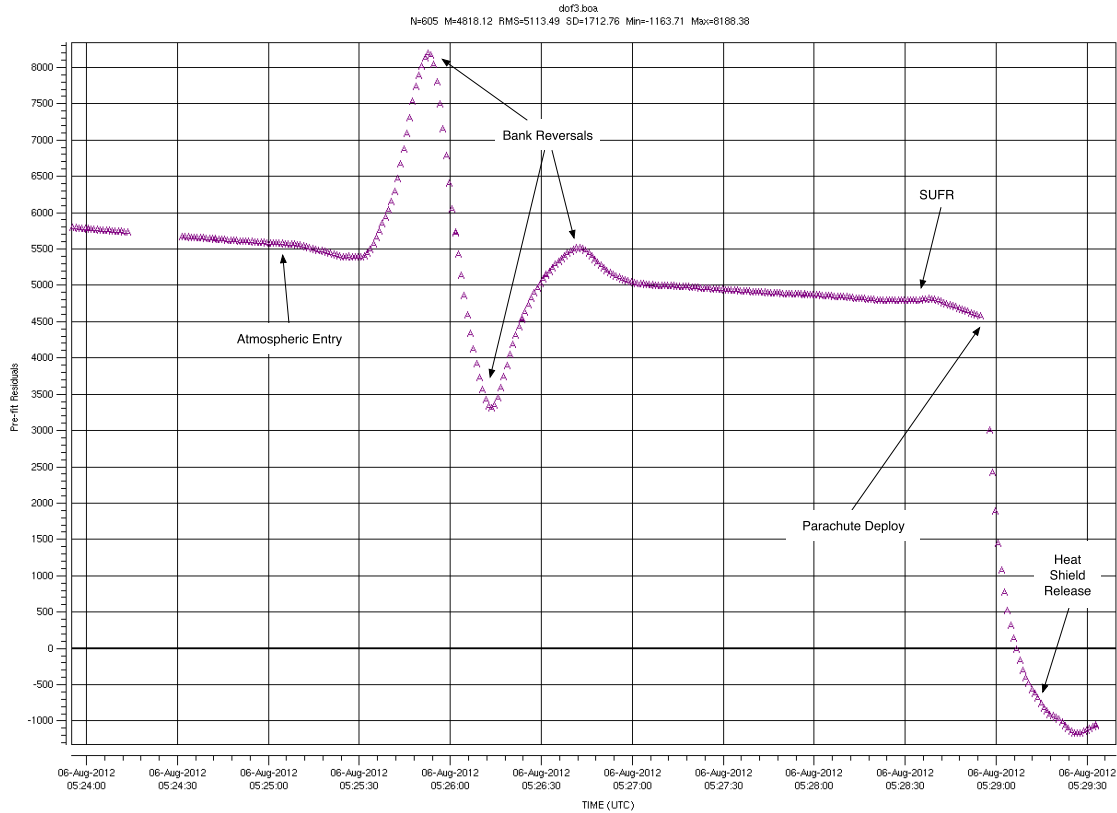


Figure 9. Real-time Doppler from entry to occultation, prediction with drag and vertical lift only. Bank reversals, SUFR, parachute deploy and HS release are noted.

- [9] Kipp, D. "Terrain safety assessment in support of the Mars Science Laboratory mission." "Aerospace Conference, 2012 IEEE," pp. 1–8. March 2012. ISSN 1095-323X. doi:10.1109/AERO.2012.6186995.
- [10] Bonfiglio, E., Adams, D., Craig, L., Spencer, D., Strauss, W., Seelos, F., Seelos, K., Arvidson, R., and Heep, T. "Landing Site Dispersion Analysis and Statistical Assessment for the Mars Phoenix Lander." "AIAA/AAS Astrodynamics Specialist Conference and Exhibit," pp. 1–19. AIAA-2008-7348, Honolulu, Hawaii, August 18-21 2008.
- [11] Martin-Mur, T., Kruizinga, G., and Wong, M. "Mars Science Laboratory Interplanetary Navigation Analysis." "22nd International Symposium on Space Flight Dynamics," Sao Jose dos Campos, Brazil, 2011.

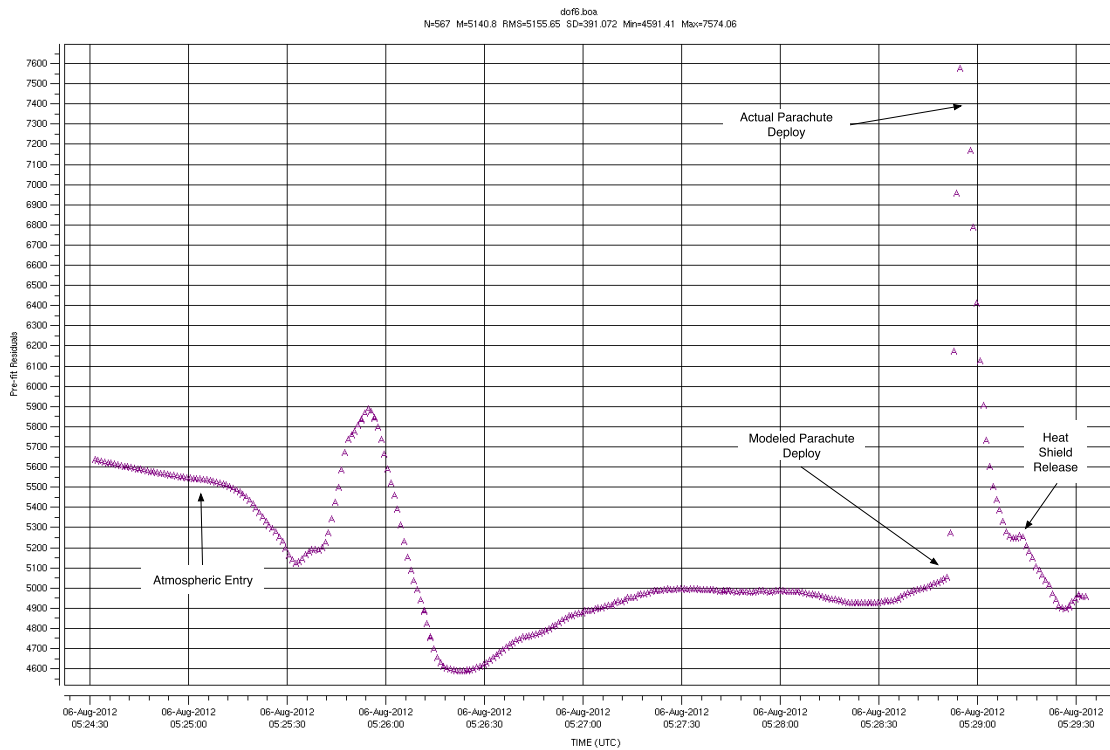


Figure 10. Real-time Doppler from entry to occultation, prediction with drag and vertical lift only. Bank reversals, SUFR, parachute deploy and HS release are noted.